2004-06-25

Mechanism Governing the Cellular Susceptibility to Secretory Phospholipase A2

Lauren Blackburn Jensen
Brigham Young University - Provo

MECHANISM GOVERNING THE CELLULAR SUSCEPTIBILITY TO SECRETORY PHOSPHOLIPASE A_2

by

Lauren B. Jensen

A thesis submitted to the faculty of

Brigham Young University

in partial fulfillment of the requirements for the degree of

Master of Science

Department of Physiology and Developmental Biology

Brigham Young University

June 2004

BRIGHAM YOUNG UNIVERSITY

GRADUATE COMMITTEE APPROVAL

of a thesis submitted by

Lauren B. Jensen

This thesis has been read by each member of the following graduate committee and by majority vote has been found to be satisfactory.

Date	John D. Bell, Chair
Date	William S. Bradshaw
Date	Allan M. Judd

BRIGHAM YOUNG UNIVERSITY

As chair of the candidate's graduate committee, I have read the thesis of Lauren B. Jensen in its final form and have found that (1) its format, citations, and bibliographical style are consistent and acceptable and fulfill university and department style requirements; (2) its illustrative materials including figures, tables, and charts are in place; and (3) the final manuscript is satisfactory to the graduate committee and is ready for submission to the university library.

_____ _____

Date

John D. Bell
Chair, Graduate Committee

Accepted for the Department

_____

James P. Porter
Department Chair, Department of Physiology and Developmental Biology

Accepted for the College

_____

R. Kent Crookston
Dean, College of Biology and Agriculture

ABSTRACT

MECHANISM GOVERNING THE CELLULAR SUSCEPTIBILITY TO SECRETORY PHOSPHOLIPASE A_2

Lauren B. Jensen
Department of Physiology and Developmental Biology
Master of Science

Secretory phospholipase A_2 ($sPLA_2$) is an important part of apoptosis and disposal of damaged and dying cells. However, healthy cells are not susceptible to attack by $sPLA_2$. Recent studies have focused on membrane properties necessary to induce susceptibility in both artificial and biological membranes. Hydrolysis of phospholipids by $sPLA_2$ requires at least two preliminary steps: first, adsorption of the enzyme to the cellular membrane, and second, movement of a phospholipid into the active site of the enzyme. We determined the effects of susceptibility on each of the two steps and determined the contributions changing the equilibrium constants have on susceptibility. The equilibrium constant for step one increased by a factor of 2 during susceptibility, while the equilibrium constant for step two increased by a factor of 4. The rise in the second equilibrium constant caused the majority of the change in hydrolysis rate seen during susceptibility; the influence of the first equilibrium constant is minimal. We

confirmed these results with adsorption studies (assessment of the first step). We additionally found that $sPLA_2$ has a high affinity for the cellular membrane and that only a small percentage (3-5%) of the membrane is covered when all adsorption sites are filled by the enzyme. We proposed a mathematical model describing the mechanism of action of $sPLA_2$, and we were able to experimentally justify the assumptions made in the model.

ACKNOWLEDGMENTS

I would like to thank Dr. John Bell for all of his effort, time, and assistance in helping me achieve this degree. I appreciate the help from the rest of my committee, Drs. William Bradshaw and Allan Judd, as well. I am very grateful to Dr. Theodore Hazlett and Susana Sanchez for providing technical assistance and access to the two-photon scanning microscope found at the Laboratory for Fluorescence Dynamics at the University of Illinois at Champaign-Urbana. I acknowledge the generous funding from the National Science Foundation and from Bioflam. Most importantly, I would like to thank my family and especially my husband, Rick Jensen, for their love, support, and encouragement during my time here.

TABLE OF CONTENTS

LIST OF TABLES

LIST OF SCHEMES

LIST OF FIGURES

INTRODUCTION

Secretory phospholipase A_2 ($sPLA_2$) is a low-molecular weight, extracellular protein involved in the inflammation process and cellular apoptosis (1-8). It has also been implicated in the pathology of septic shock (9). During cellular trauma, $sPLA_2$ adsorbs to the cellular membrane and hydrolyzes phospholipids at the *sn*-2 position, creating fatty acids and lysophospholipids. The byproducts of phospholipid hydrolysis are further converted to inflammation factors (leukotrienes, arachidonic acid, etc.). Healthy cells resist attack by $sPLA_2$, but damaged or dying cells are susceptible to hydrolysis (6-11). In this manner $sPLA_2$ is able to dispose of phospholipids of damaged and dying cells, but healthy cells are not affected.

Initial studies using artificial vesicles have shown that the enzyme is able to adsorb to membranes and hydrolyze the phospholipids (12,13). Additional experiments have described the properties that make artificial membranes susceptible to attack by $sPLA_2$: the lipid composition of the membrane and the concentration of hydrolysis products, temperature, vesicle curvature (14-18). However, these experiments do not necessarily represent enzyme-membrane interactions in biological systems. Erythrocytes are a simple model for studying biological membrane susceptibility to $sPLA_2$ as they resist attack by $sPLA_2$ when healthy but changes in the membrane lead to susceptibility (11,19).

Calcium has a dual role during membrane attack by $sPLA_2$. Extracellular calcium serves as a cofactor for the enzyme and is necessary for hydrolysis to occur (20). Intracellular calcium affects the properties of the membrane, influencing susceptibility to the enzyme (21). We will be exploiting this duality to control susceptibility and isolate

certain steps in the hydrolysis process. Barium interferes with the calcium as a cofactor (22), but still allows intracellular calcium to change the membrane properties essential for susceptibility. Ionomycin is a calcium ionophore that increases intracellular calcium, which we will use to influence the membrane properties to increase susceptibility (11). Ionomycin does not affect the function of extracellular calcium as an enzyme cofactor.

The events leading to hydrolysis of phospholipids by $sPLA_2$ can be described by a two-step model (shown in Scheme 1): first, adsorption of the enzyme to the cellular membrane; and second, movement of a phospholipid into the active site. Changes in either or both steps may lead to increased susceptibility. Our ultimate goal is to produce a mathematical model describing the mechanism of action of $sPLA_2$ and how susceptibility affects the action of the enzyme. Unpublished data from our lab showed that changing the temperature affects susceptibility through both steps in the two-step model. Additional unpublished data from our lab showed that increasing intracellular calcium concentration increases the tendency of a phospholipid to move out of the membrane and into the active site of the enzyme (the second step).

We studied the influence of increasing susceptibility on each step of the model by changing intracellular calcium concentration (by treating the cells with ionomycin). We found that the second step was greatly increased during susceptibility, while step one was only slightly changed. We were able to validate the results for step one: the effect of ionomycin treatment on adsorption individually was not significantly different than control. Additionally, we justified experimentally the assumptions made in our mathematical model. Finally, we quantified the number of $sPLA_2$ adsorption sites on the cell surface.

MATERIALS AND METHODS

Materials

Erythrocytes were obtained from healthy individuals receiving blood tests during physical examinations at the Brigham Young University Student Health Center. The samples were stored overnight at 4 ºC in EDTA vacutainers from which patient identification was removed. The storage conditions did not influence the results (11). Erythrocytes were isolated by centrifugation, and resuspended to the original hematocrit in modified balanced salt solution (MBSS; 134 mM NaCl, 6.2 mM KCl, 1.6 mM $CaCl_2$, 1.2 mM $MgCl_2$, 18 mM HEPES, 13.6 mM glucose, pH 7.4 at 37 ºC), high-barium, low-calcium, low-magnesium medium (LCBM; 134 mM NaCl, 6.2 mM KCl, 1.6 mM $BaCl_2$, 18 mM HEPES, 13.6 mM glucose, pH 7.4 at 37 ºC) or high-barium medium (BMBSS; 134 mM NaCl, 6.2 mM KCl, 6.4 mM $BaCl_2$, 1.6 mM $CaCl_2$, 1.2 mM $MgCl_2$, 18 mM HEPES, 13.6 mM glucose, pH 7.4 at 37 ºC).

Secretory PLA_2 was isolated from the venom of *Agkistrodon piscivorus piscivorus* according to published procedure (23). This form of $sPLA_2$ represents a reliable model for the human forms of the enzyme (9,11). Stock solutions of the enzyme (1.15 mg/ml, 1.0 mg/ml, 0.77 mg/ml, and 0.1 mg/ml) were prepared in 50 mM KCl with 3 mM NaN_3 and stored at 4 ºC.

Acrylodan-labeled fatty acid-binding protein (ADIFAB) was obtained from Molecular Probes (Eugene, OR). Ionomycin was purchased from Calbiochem (La Jolla, CA) and dissolved in dimethyl sulfoxide (DMSO) at a stock concentration of 120 µM. Fluorescamine was purchased from Sigma (St. Louis, MO) and dissolved in acetone at a stock solution of 3.0 mg/ml.

Methods

Membrane hydrolysis by $sPLA_2$ – Release of free fatty acids from erythrocytes was assayed with ADIFAB (65 nM final concentration, excitation: 390 nm, emission: 432 nm and 505 nm). Washed erythrocytes were suspended in 2 ml MBSS in a fluorometer sample cell to a final density of approximately $1\text{-}2\times10^6$ erythrocytes per ml and equilibrated at 37 ºC. Fluorescence data were acquired on a photon-counting spectrofluorometer (Fluoromax (Jobin Yvon Horiba, Edison, NJ, USA)). After initiating data acquisition, ADIFAB was added at 30 s, followed by ionomycin (300 nM) or DMSO at 130 s, and $sPLA_2$ (21 nM-700 nM) at 730 s. Hydrolysis results were quantified by calculation of generalized polarization (GP) and fit as described (11) using statistical software (Prism 3.0 or Prism 4.0). The initial hydrolysis rate was approximated as the amount of reaction product generated at 20 s following $sPLA_2$ (using coefficient values from the nonlinear regression results).

Fluorescamine labeling – Fluorescamine (180 μM final concentration, excitation: 390 nm, emission: 485 nm) was added to $sPLA_2$ (1.4 μM) and allowed to react at 37 ºC. Progression of the labeling reaction was monitored by fluorescence spectroscopy as described above.

Two-photon microscopy – Scanning two-photon excitation microscopy images were collected on an Axiovert 35 inverted microscope (Zeiss, Thornwood, NY, USA) at the Laboratory for Fluorescence Dynamics (Urbana, IL) as described previously (24). The excitation source was a titanium-sapphire laser (Coherent, Palo Alto, CA, USA) tuned to 780 nm and pumped by a frequency-doubled Nd:vandate laser. Power was set at 80-100 mW. Secretory PLA_2 was labeled with fluorescamine as described above.

Washed erythrocytes were mixed with 1 ml BMBSS in a temperature-controlled microscopy dish (approximately 1-2×10^6 erythrocytes per ml) and allowed to equilibrate at 37 ºC. Ionomycin (300 nM) or DMSO was added, and the mixture was incubated at least 5 min. To quantify adsorption, images were acquired at multiple time points before and after addition of fluorescamine-labeled $sPLA_2$. Total fluorescence intensity (after subtraction of a background threshold) was measured for each image. Slopes of the fluorescence trends were calculated by linear regression using image number as the independent variable and intensity as the dependent variable. The difference between the slopes of increasing fluorescence before and after addition of labeled enzyme were calculated and compared as a function of enzyme concentration.

Adsorption site quantification – Secretory PLA_2 was labeled with fluorescamine as described above. Washed erythrocytes were suspended in 1 ml LCBM in a microcentrifuge tube to a final density of approximately 1-2×10^6 erythrocytes per ml. Fluorescamine-labeled $sPLA_2$ (70 nM) was added, and the mixture was incubated at least 10 min at 37 º C. The mixture was centrifuged (G force: 15,000 g units) for 15 s, and the pellet was washed and resuspended in 2 ml LCBM. Fluorescence data were acquired on a Fluoromax. Control experiments were performed without erythrocytes or without fluorescamine-labeled $sPLA_2$ to measure noise.

DESCRIPTION OF MODEL

The model describing the action of $sPLA_2$ on the surface of membranes is shown in Scheme 1. The rate of hydrolysis (*dP/dt*) is given by the following:

$$\frac{dP}{dt} = k_{cat} E_B^S \tag{1}$$

Experiments were conducted in which the concentration of cells and, therefore, the total number of binding sites for the enzyme (M_{ST}) were kept constant. The equilibrium constants (K_1 and K_2) are defined as follows:

$$K_1 = \frac{E_B}{(E)(M_S)} \tag{2}$$

$$K_2 = \frac{E_B^S}{(E_B)(S)} \tag{3}$$

If we confine our analysis to the initial part of the hydrolysis time course, then *S* can be assumed to be a constant mole fraction of M_{ST} (S_0). Since S_0 is a constant, the apparent value of K_2 (K_2^*) is proportional to K_2 and can be used in our calculations:

$$K_2^* = \frac{E_B^S}{E_B} \tag{4}$$

The distribution of membrane binding sites between occupied and unoccupied states is given by:

$$M_{ST} = M_S + E_B + E_B^S \tag{5}$$

If we assume that only a small fraction of added enzyme adsorbs to the cell surface, then *E* can be approximated by the total enzyme concentration, E_T. This assumption was verified by binding experiments described in the next section. An explicit description of the initial hydrolysis rate can be obtained by combining equations 1, 2, and 4:

$$\frac{dP}{dt} = \frac{\alpha E_T K_1 K_2^*}{1 + E_T K_1 + E_T K_1 K_2^*} \tag{6}$$

where α is proportional to $k_{cat} M_{ST}$.

RESULTS AND DISCUSSION

We assumed that changing membrane properties that lead to susceptibility to attack by $sPLA_2$ affects either or both of the two steps prior to hydrolysis described in Scheme 1. The initial hydrolysis rate of cellular membranes can be used to find the change in equilibrium constants during susceptibility. Assessment of adsorption (step one) can validate the hydrolysis kinetics results. Quantification of the number of adsorption sites can justify the assumptions made in the model, along with giving us more details about the mechanism of action of $sPLA_2$.

Hydrolysis kinetics

The fluorescent fatty acid-binding protein, ADIFAB, is a useful probe for studying hydrolysis, since the shape of its emission spectrum changes upon binding to free fatty acids (products of phospholipid hydrolysis). ADIFAB is excited at 390 nm and emits with a peak at 432 nm when free in solution. However, the emission curve shifts to 505 nm when ADIFAB is bound to fatty acids. Generalized polarization (GP) is a comparison between the emission curves of bound and unbound ADIFAB and is determined using equation 7.

$$GP = \frac{b - a}{b + a} \tag{7}$$

where a is the emission intensity at 432 nm and b is the intensity at 505 nm. An increase in GP indicates a shift toward 505 nm and, therefore, an increase in hydrolysis of phospholipids. The time courses of hydrolysis were fit to equation 8 using nonlinear regression.

$$y = A(1 - e^{-Bt}) + C(1 - e^{-Dt}) + Et + F \tag{8}$$

where y is the amount of hydrolysis at time t. Figure 1 shows a time course of hydrolysis of phospholipids using this probe at 21 nM (black squares) and 700 nM (red triangles) $sPLA_2$. As can be seen, $sPLA_2$ causes hydrolysis of phospholipids within the range of concentrations examined.

The model assumes that the total number of binding sites and total initial substrate concentration remain the same at all experimental conditions. However, the data in Figure 1 seem to violate this assumption. The time courses reached a "plateau" phase within 200 s that appear to become parallel, suggesting that the total amount of substrate available for hydrolysis varies with enzyme concentration. To explore this possibility, we repeated the experiments of Figure 1 for much longer periods of time (Figure 2). These long-term experiments showed that the "plateau" phase of hydrolysis seen at the end of the time courses in Figure 1 actually represented slow hydrolysis that continued for multiple hours. Consequently, at true completion of the reaction, the time courses did, in fact, converge at 70 nM (black) and 700 nM (red). Thus, these experiments validated the model's assumption that the total amount of substrate available for hydrolysis per cell is constant.

Ionomycin treatment changed the shape of the hydrolysis time course. Cells were treated with the ionophore 10 min prior to addition of 21 nM (black squares) or 700 nM (red triangles) $sPLA_2$ (Figure 3). The amount of hydrolysis was determined by ADIFAB. Hydrolysis increased rapidly initially and required much less time to approach a true plateau at which the hydrolysis curves at both high and low concentrations of enzyme converged.

Initial hydrolysis rate changed as a function of the concentration of $sPLA_2$ (Figure 1, Figure 3). Cells were treated with or without ionomycin before addition of various concentrations (21 nM, 70 nM, 210 nM, or 700 nM) of $sPLA_2$. Hydrolysis was measured with ADIFAB and hydrolysis curves fit to equation 8. The values of the coefficients were used to determine the rate of hydrolysis at 20 s. Twenty seconds was determined to be the earliest time at which hydrolysis measurements are reliable. Accordingly, this time point was defined as "initial hydrolysis" and used for comparison among various concentrations. Figure 4 shows the results of this comparison—red triangles: initial hydrolysis rates of ionomycin-treated cells; black squares: initial hydrolysis rates of control (untreated) cells. The hydrolysis rate of cellular membranes increased significantly with ionomycin treatment at all $sPLA_2$ concentrations: a two-way analysis of variance showed that treatment with ionomycin accounted for 34.3% of the total variation ($p<0.0001$) and increasing the enzyme concentration accounted for 14.1% of the total variation ($p=0.0079$). The interaction between the two terms was not significant.

The relationship between hydrolysis rate and the equilibrium constants was mathematically defined in *Description of Model* and can be used to determine the change in the equilibrium constants upon an increase in susceptibility for both steps in our model. Global analysis was performed on the data collected for Figure 4 using equation 6. As stated earlier, α is a constant that represents k_{cat}, or hydrolysis of the phospholipid once it has moved into the active site. We assumed that α was not dependent upon the level of membrane susceptibility because we assumed that once the phospholipid has moved out of the membrane and into the active site of the enzyme, it is no longer affected by the membrane properties that determine susceptibility. We, therefore, constrained α to

remain equal between the two conditions (ionomycin-treated cells and control cells). Table 1 and Figure 5A show the results of the global analysis (red triangles: ionomycin-treated cells; black squares: control cells). Changing the membrane properties by increasing intracellular calcium amplified the equilibrium constant for the first step (K_1) by a factor of two and the equilibrium constant for the second step (K_2^*) by a factor of four. In other words, the affinity of $sPLA_2$ for the cellular membrane doubled and the probability of a phospholipid moving into the active site of the enzyme quadrupled. Figure 5B shows the effects of this increase in the individual steps. The solid black line (and black squares) indicates the initial hydrolysis rate of control cells; the solid red line (and red triangles) indicates the initial hydrolysis rate of ionomycin-treated cells. Increasing only K_1 by the factor of two is indicated by the dotted line. The dotted line very closely resembles the solid black line and is within the error bars of the black squares. Increasing only K_2^* by the factor of four is indicated by a dashed line. The dashed line very closely resembles the solid red line and is within the error bars of the red triangles. Thus, the increase in K_2^* contributes the majority of the effect of susceptibility, while the increase in K_1 merely refines the curve.

Step 1: Adsorption kinetics

In order to study the adsorption of $sPLA_2$ to the cellular membrane, we labeled the enzyme with fluorescamine, a fluorescent probe that covalently binds to primary amines (25). Fluorescamine is fluorescent only when attached to amines; the fluorescence of residual probe is destroyed by reaction of free fluorescamine with water. Fluorescamine is excited at 390 nm and emits at 485 nm. Because labeling of $sPLA_2$ requires covalent modification, we conducted experiments to determine if this covalent

modification changed the behavior of the enzyme. Various concentrations of fluorescamine-labeled $sPLA_2$ (17 nM, 35 nM, and 70 nM) were added to ionomycin-treated or control erythrocytes. Hydrolysis was measured with ADIFAB and hydrolysis curves fit to equation 8. Unfortunately, ADIFAB and fluorescamine are excited and emit at the nearly identical wavelengths, changing the overall emission curve and affecting ADIFAB GP. Additionally, $sPLA_2$ binds to the walls of the cuvette over time, decreasing the amount of fluorescamine fluorescence. These issues complicated interpretation of the results. Figure 6A shows the results of a hydrolysis time course at 70 nM $sPLA_2$ (red: ionomycin-treated cells; black: control cells). Hydrolysis did occur and was greater in susceptible (ionomycin-treated) cells than in control cells. This result was made more apparent by considering the difference between the data from control and ionomycin-treated samples at 17 nM (black), 35 nM (blue), and 70 nM (red) $sPLA_2$ (Figure 6B). As in Figure 4, ionomycin-treated cells were initially hydrolyzed at a faster rate than control cells (seen by a positive difference) at all enzyme concentrations. Additionally, hydrolysis by fluorescamine-labeled $sPLA_2$ increased with increasing enzyme concentration (Figure 6B), similar to the results seen in Figure 3. Hence, covalent labeling of $sPLA_2$ with fluorescamine did not change the enzyme's general behavior toward cell membranes.

To determine the nature of adsorption of the enzyme to a cellular membrane, we observed fluorescence before and after adding fluorescamine-labeled $sPLA_2$ (Figure 7). Panel A is a field of untreated cells; Panel B is the same field of cells after adding 35 nM fluorescamine-labeled $sPLA_2$; Panel C is the same field 6 min after adding 2.9 μM unlabeled $sPLA_2$. The amount of fluorescence did not decrease after adding unlabeled

enzyme, indicating that desorption of $sPLA_2$ from the cellular membrane was very slow or that the enzyme bound nonspecifically. To determine the specificity of binding, we reversed the order of addition: 700 nM unlabeled $sPLA_2$ 21 min before 70 nM fluorescamine-labeled $sPLA_2$. Panel D shows the results of this order of addition: the fluorescamine-labeled $sPLA_2$ was not able to compete for the adsorption sites already filled by unlabeled enzyme. Thus, adsorption of $sPLA_2$ to the cellular membrane appeared to be specific and long-lived.

The influence of increasing membrane susceptibility on adsorption of the enzyme to the cell surface was also viewed through two-photon microscopy. We treated cells with or without ionomycin and acquired multiple images of the same field before and after addition of 14 nM or 70 nM fluorescamine-labeled $sPLA_2$. Total intensity was calculated for each image and plotted as a function of total number of scans. The slope for increasing fluorescence was determined through linear regression. The fluorescence slope before addition of labeled enzyme constituted an increase in autofluorescence from the power of the microscope. The fluorescence slope after addition of labeled enzyme, if higher than the fluorescence slope before addition of labeled enzyme, signified adsorption of labeled enzyme to the cellular membrane. We determined the normalized difference between the fluorescence slopes before and after addition of labeled enzyme (see equation 9).

$$\frac{S_B - S_A}{S_B} \tag{9}$$

where S_B represents the fluorescence slope before addition of labeled enzyme and S_A represents the fluorescence slope after addition of labeled enzyme. The normalized difference was plotted as a function of increasing enzyme concentration (Figure 8—red

triangles: ionomycin-treated cells; black squares: control cells). The amount of adsorption did not significantly increase in susceptible cells compared to control cells. Two-way analysis of variance revealed that the effect of enzyme concentration explained 48.8% of the variation seen ($p=0.013$), while the effects of ionomycin could rationalize only 1.2% of the variation ($p=0.57$). Thus, the increase in fluorescence was accounted for by the amount of enzyme added; ionomycin did not significantly increase the adsorption of $sPLA_2$ to the cellular membrane. The interaction between two terms was almost significant ($p=0.2$); a larger sample size may lead to a significant interaction term. These data justify our conclusion from the global analysis of hydrolysis kinetics that a change in K_I does not significantly contribute to susceptibility.

Quantification of the number of $sPLA_2$ adsorption sites on the cell surface

Similar experiments were used to quantify the number of $sPLA_2$ binding sites on the cellular membrane. We incubated cells in a "calcium-free" (barium replaced calcium) buffer with 70 nM fluorescamine-labeled $sPLA_2$. We centrifuged the suspension and measured the fluorescence of the washed pellet. Control experiments were conducted without erythrocytes or without labeled enzyme to measure background noise. The amount of fluorescence in the washed pellet is proportional to the amount of labeled enzyme adsorbed to the cellular membrane. The potential number of binding sites was determined by comparing the total surface area of the enzyme to the total surface area of an erythrocyte and assuming that the surface of the erythrocyte was covered by enzyme (26,27). Table 2 compares the measured number of binding sites to the potential number of binding sites. Our measurements suggested that only 2-4% of the erythrocyte membrane is covered by $sPLA_2$.

Our results estimated that 2.68×10^5 enzymes are adsorbed to each cell. We added approximately 4.0×10^6 cells per 2 ml cuvette, totaling 1.072×10^{12} enzymes adsorbed per 2 ml cuvette. When we added 700 nM $sPLA_2$ to the 2 ml cuvette, we added approximately 8.43×10^{14} enzyme molecules per 2 ml cuvette. Thus, 0.172% of the enzyme added was adsorbed to the cells. Even if the cell were completely covered with $sPLA_2$, 3.4×10^{13} enzymes, or 4.03% of the total enzyme added, would be adsorbed per sample. Thus, our assumption that E can be approximated by E_T is justified.

FINAL COMMENTS

Our ultimate goal is to define a mathematical model that describes the mechanism of action of $sPLA_2$ and explains susceptibility within that mechanism of action. These results suggest that our two-step model applies to biological systems. We were able to validate the assumption that M_{ST} remains constant and that E can be approximated by E_T. Additionally, we were able to resolve the contributions of each step (K_1 and K_2^*) on the level of cellular susceptibility using our model. This study argues that the model is sufficient to explain the mechanism of action of $sPLA_2$ toward both resistant and susceptible membranes.

Reference List

1. Uhl, W., Buchler, M., Nevalainen, T. J., Deller, A., and Beger, H. G. (1990) Serum phospholipase A2 in patients with multiple injuries *J.Trauma* **30,** 1285-1290
2. Nevalainen, T. J., Gronroos, J. M., and Kortesuo, P. T. (1993) Pancreatic and synovial type phospholipases A2 in serum samples from patients with severe acute pancreatitis *Gut* **34,** 1133-1136
3. Haapamaki, M. M., Gronroos, J. M., Nurmi, H., Alanen, K., Kallajoki, M., and Nevalainen, T. J. (1997) Gene expression of group II phospholipase A2 in intestine in ulcerative colitis *Gut* **40,** 95-101
4. Andersen, S., Sjursen, W., Laegreid, A., Volden, G., and Johansen, B. (1994) Elevated expression of human nonpancreatic phospholipase A2 in psoriatic tissue *Inflammation* **18,** 1-12
5. Nag, M. K., Deshpande, Y. G., Li, A., Beck, D., and Kaminski, D. L. (1995) Lysophosphatidylcholine-stimulated protein and glycoprotein production by human gallbladder mucosal cells *Dig.Dis.Sci.* **40,** 1990-1996
6. Wilson, H. A., Allred, D. V., O'Neill, K., and Bell, J. D. (2000) Activities and interactions among phospholipases A2 during thapsigargin- induced S49 cell death *Apoptosis.* **5,** 389-396
7. Nielson, K. H., Olsen, C. A., Allred, D. V., O'Neill, K. L., Burton, G. F., and Bell, J. D. (2000) Susceptibility of S49 lymphoma cell membranes to

hydrolysis by secretory phospholipase A(2) during early phase of apoptosis *Biochim.Biophys.Acta* **1484,** 163-174

8. Atsumi, G., Murakami, M., Tajima, M., Shimbara, S., Hara, N., and Kudo, I. (1997) The perturbed membrane of cells undergoing apoptosis is susceptible to type II secretory phospholipase A2 to liberate arachidonic acid *Biochim.Biophys.Acta* **1349,** 43-54
9. Wilson, H. A., Waldrip, J. B., Nielson, K. H., Judd, A. M., Han, S. K., Cho, W., Sims, P. J., and Bell, J. D. (1999) Mechanisms by which elevated intracellular calcium induces S49 cell membranes to become susceptible to the action of secretory phospholipase A2 *J.Biol.Chem.* **274,** 11494-11504
10. Kudo, I., Murakami, M., Hara, S., and Inoue, K. (1993) Mammalian non-pancreatic phospholipases A2 *Biochim.Biophys.Acta* **1170,** 217-231
11. Smith, S. K., Farnbach, A. R., Harris, F. M., Hawes, A. C., Jackson, L. R., Judd, A. M., Vest, R. S., Sanchez, S., and Bell, J. D. (2001) Mechanisms by which intracellular calcium induces susceptibility to secretory phospholipase A2 in human erythrocytes *J.Biol.Chem.* **276,** 22732-22741
12. Berg, O. G., Yu, B. Z., Rogers, J., and Jain, M. K. (1991) Interfacial catalysis by phospholipase A2: determination of the interfacial kinetic rate constants *Biochemistry* **30,** 7283-7297

13. Jain, M. K. and Berg, O. G. (1989) The kinetics of interfacial catalysis by phospholipase A2 and regulation of interfacial activation: hopping versus scooting *Biochim.Biophys.Acta* **1002,** 127-156

14. Ghomashchi, F., Yu, B. Z., Berg, O., Jain, M. K., and Gelb, M. H. (1991) Interfacial catalysis by phospholipase A2: substrate specificity in vesicles *Biochemistry* **30,** 7318-7329

15. Honger, T., Jorgensen, K., Biltonen, R. L., and Mouritsen, O. G. (1996) Systematic relationship between phospholipase A2 activity and dynamic lipid bilayer microheterogeneity *Biochemistry* **35,** 9003-9006

16. Gheriani-Gruszka, N., Almog, S., Biltonen, R. L., and Lichtenberg, D. (1988) Hydrolysis of phosphatidylcholine in phosphatidylcholine-cholate mixtures by porcine pancreatic phospholipase A2 *J.Biol.Chem.* **263,** 11808-11813

17. Henshaw, J. B., Olsen, C. A., Farnbach, A. R., Nielson, K. H., and Bell, J. D. (1998) Definition of the specific roles of lysolecithin and palmitic acid in altering the susceptibility of dipalmitoylphosphatidylcholine bilayers to phospholipase A2 *Biochemistry* **37,** 10709-10721

18. Bell, J. D., Baker, M. L., Bent, E. D., Ashton, R. W., Hemming, D. J., and Hansen, L. D. (1995) Effects of temperature and glycerides on the enhancement of Agkistrodon piscivorus piscivorus phospholipase A2 activity by lysolecithin and palmitic acid *Biochemistry* **34,** 11551-11560

19. Best, K., Ohran, A., Hawes, A., Hazlett, T. L., Gratton, E., Judd, A. M., and Bell, J. D. (2002) Relationship between Erythrocyte Membrane Phase

Properties and Susceptibility to Secretory Phospholipase A2 *Biochemistry* **41,** 13982-13988

20. Yu, B. Z., Berg, O. G., and Jain, M. K. (1993) The divalent cation is obligatory for the binding of ligands to the catalytic site of secreted phospholipase A2 *Biochemistry* **32,** 6485-6492
21. Vest, R. S., Gonzales, L. J., Permann, S. A., Spencer, E., Hansen, L. D., Judd, A. M., and Bell, J. D. (2004) Divalent cations increase lipid order in erythrocytes and susceptibility to secretory phospholipase A2 *Biophys.J.* **86,** 2251-2260
22. Jain, M. K., Tao, W. J., Rogers, J., Arenson, C., Eibl, H., and Yu, B. Z. (1991) Active-site-directed specific competitive inhibitors of phospholipase A2: novel transition-state analogues *Biochemistry* **30,** 10256-10268
23. Maraganore, J. M., Merutka, G., Cho, W., Welches, W., Kezdy, F. J., and Heinrikson, R. L. (1984) A new class of phospholipases A2 with lysine in place of aspartate 49. Functional consequences for calcium and substrate binding *J.Biol.Chem.* **259,** 13839-13843
24. Parasassi, T., Gratton, E., Yu, W. M., Wilson, P., and Levi, M. (1997) Two-photon fluorescence microscopy of laurdan generalized polarization domains in model and natural membranes *Biophys.J.* **72,** 2413-2429
25. Udenfriend, S., Stein, S., Bohlen, P., Dairman, W., Leimgruber, W., and Weigele, M. (1972) Fluorescamine: a reagent for assay of amino acids, peptides, proteins, and primary amines in the picomole range *Science* **178,** 871-872

26. Evans, E. and Fung, Y. C. (1972) Improved measurements of the erythrocyte geometry *Microvasc.Res.* **4,** 335-347

27. Arni, R. K. and Ward, R. J. (1996) Phospholipase A2--a structural review *Toxicon* **34,** 827-841

Table 1: Global analysis of effect of ionomycin on initial hydrolysis rate.

Values of K_1, K_2, and α for susceptible and control erythrocytes obtained during the global analysis for Figure 5.

Table 1

	Control cells	Ionomycin-treated cells
α	0.08965	0.08965
K_1 (nM^{-1})	0.008508	0.01746
K_2^*	0.7099	2.888

Table 2. Quantification of the number of adsorption sites for $sPLA_2$ on erythrocyte membranes. Theoretical binding sites assume complete coating of the cell by enzyme as calculated by the ratio of the surface area of the cell to the surface area of $sPLA_2$. The measured number of sites was obtained by quantifying the amount of fluorescamine-labeled $sPLA_2$ retained following centrifugation and washing of cells labeled as shown in Figure 7.

Table 2

	Number of $sPLA_2$ binding sites per cell	Percentage of cell covered by $sPLA_2$
theoretical	$8.5*10^6$	100%
measured	$2.7*10^5$ ($SE=6.8*10^4$)	2-4%

FIGURE LEGENDS

Scheme 1: Description of the two-step model. Secretory PLA_2 requires at least two steps prior to hydrolysis: first, free enzyme (E) adsorbs to adsorption sites on the membrane (M_S) to become bound enzyme (E_B); and second, a phospholipid (S) moves from the membrane into the active site of the enzyme (E_B^S). Ultimately, hydrolysis of the phospholipid occurs, creating free fatty acid and lysophospholipid (P). The enzyme remains bound. Equilibrium constants for the two steps are given as K_1 and K_2 and the hydrolysis rate constant is given by k_{cat}.

Figure 1: Effect of enzyme concentration on the early time courses of erythrocyte hydrolysis by $sPLA_2$. Control erythrocytes were incubated with 21 nM (black squares) or 700 nM (red triangles) $sPLA_2$ for 300 s, and hydrolysis was assayed by ADIFAB fluorescence as described in *Materials and Methods*. Hydrolysis was quantified as GP and curves were obtained with nonlinear regression (as described in the text). Each datum represents the mean ± S.E. of data from seven blood samples.

Figure 2: Extended time courses of erythrocyte hydrolysis at high and low concentrations of $sPLA_2$. Control erythrocytes were incubated with 70 nM (black) or 700 nM (red) $sPLA_2$ for 1 to 3 h and hydrolysis assayed as described for Figure 1.

Figure 3: Effect of ionomycin treatment on time courses of erythrocyte hydrolysis at high and low concentrations of $sPLA_2$. The experiments of Figure 1 were repeated using ionomycin-treated erythrocytes (see *Materials and Method*). Each datum represents the mean ± S.E. of data from seven blood samples.

Figure 4: Effect of ionomycin treatment on the enzyme-concentration dependence of the initial rate of hydrolysis of erythrocytes. Various concentrations

(21 nM, 70 nM, 210 nM, and 700 nM) $sPLA_2$ were added to ionomycin-treated (red triangles) or control erythrocytes (black squares) and hydrolysis assessed as in Figure 1. The initial rates of hydrolysis were ascertained from time courses such as those shown in Figures 1 and 3 and analyzed as explained in *Materials and Methods*. Each datum represents the mean ± S.E. of data from seven blood samples.

Figure 5: Global Analysis of effect of ionomycin on initial hydrolysis rate. The data obtained for Figure 4 were analyzed with global analysis (as described in the text) based on the relationship between hydrolysis rate and equilibrium constants (mathematically defined in *Description of the Model*). *Panel A*: Hydrolysis curves obtained by global analysis with α held constant (red: ionomycin-treated erythrocytes; black: control erythrocytes). *Panel B*: The contributions to susceptibility of increasing each equilibrium constant separately (red: ionomycin-treated erythrocytes; solid black: control erythrocytes; dotted black: increasing K_1 by a factor of 2; dashed black: increasing K_2 by a factor of 4).

Figure 6: Control for possible effects of fluorescamine labeling on behavior of $sPLA_2$. Fluorescamine-labeled $sPLA_2$ was added to ionomycin-treated or control erythrocytes and hydrolysis was assayed as described in Figure 1. *Panel A*: Sample time course of hydrolysis (red: ionomycin-treated erythrocytes; black: control erythrocytes). *Panel B*: Differences between hydrolysis of ionomycin-treated erythrocytes and hydrolysis of control erythrocytes at 18 nM (black), 35 nM (blue), and 70 nM (red) $sPLA_2$.

Figure 7: Visualization of adsorption of fluorescamine-labeled $sPLA_2$ to erythrocyte membranes with two-photon microscopy. *Panel A*: baseline fluorescence

prior to addition of labeled $sPLA_2$. *Panel B*: same sample following addition of 35 nM fluorescamine-labeled $sPLA_2$. *Panel C*: same sample as B 6 min following addition of 2.9 μM unlabeled $sPLA_2$. *Panel D*: new sample with 700 nM unlabeled $sPLA_2$ added 21 min prior to 70 nM labeled $sPLA_2$. Experiments were conducted in buffer containing barium to inhibit extraction and hydrolysis of membrane phospholipids using the two-photon procedure described in *Materials and Methods*.

Figure 8: Effect of ionomycin treatment on adsorption of $sPLA_2$ to erythrocyte membranes. Various concentrations (0, 14 nM, or 70 nM) of fluorescamine-labeled $sPLA_2$ were added to ionomycin-treated or control erythrocytes and images acquired as in Figure 7. The amount of fluorescence attributed to adsorption of labeled $sPLA_2$ was quantified as described in *Materials and Methods*. Two-way analysis of variance revealed that the effect of enzyme concentration was significant (p = 0.013), but the effects of ionomycin were not (p = 0.57). Each datum represents the mean ± S.E., n = 1 to 4 blood samples.

Scheme 1

$$E + M_S \underset{K_1}{\rightleftharpoons} E_B \overset{S}{\underset{K_2}{\rightleftharpoons}} E_B{}^S \xrightarrow[k_{cat}]{} E_B + P$$

Figure 1

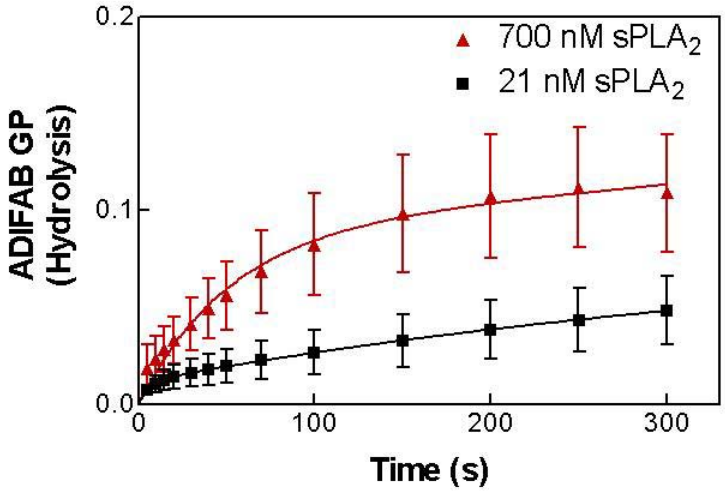
0.2
0.1
0.0
0
100
200
300
ADIFAB GP
(Hydrolysis)
Time (s)
700 nM sPLA2
21 nM sPLA2

Figure 2

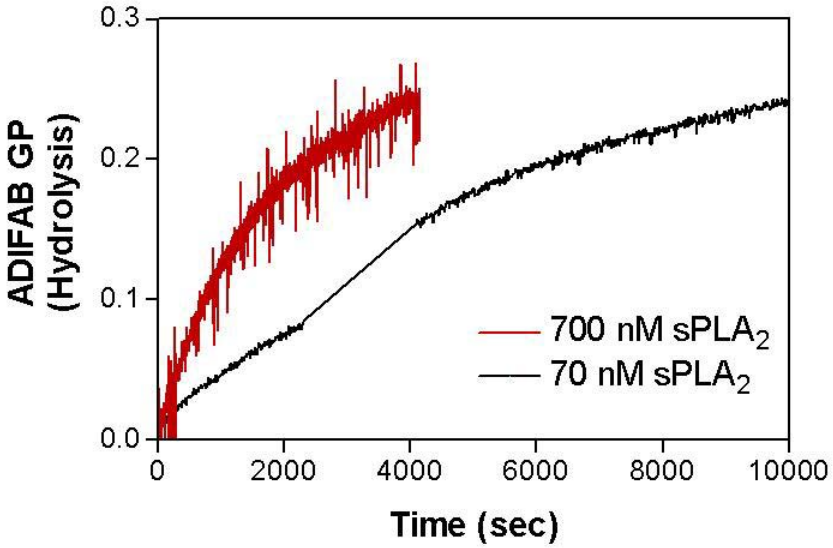
ADIFAB GP
(Hydrolysis)
0.3
0.2
0.1
0.0
0
2000
4000
6000
8000
10000
Time (sec)
700 nM sPLA2
70 nM sPLA2

Figure 3

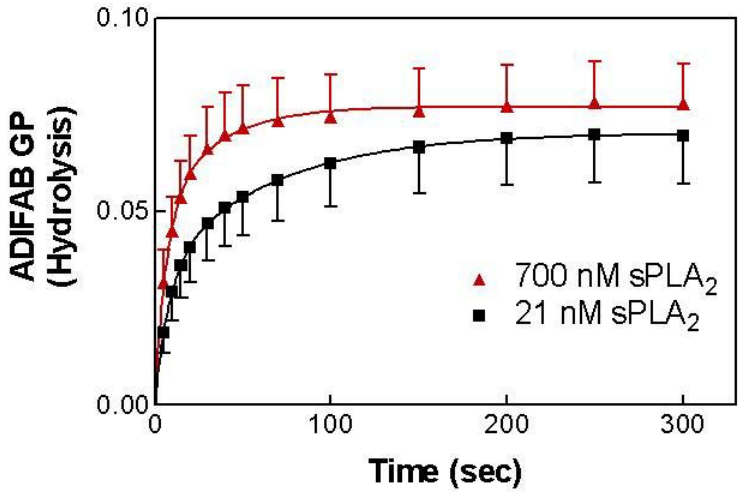
0.10
0.05
0.00
0
100
200
300
ADIFAB GP
(Hydrolysis)
Time (sec)
700 nM sPLA2
21 nM sPLA2

Figure 4

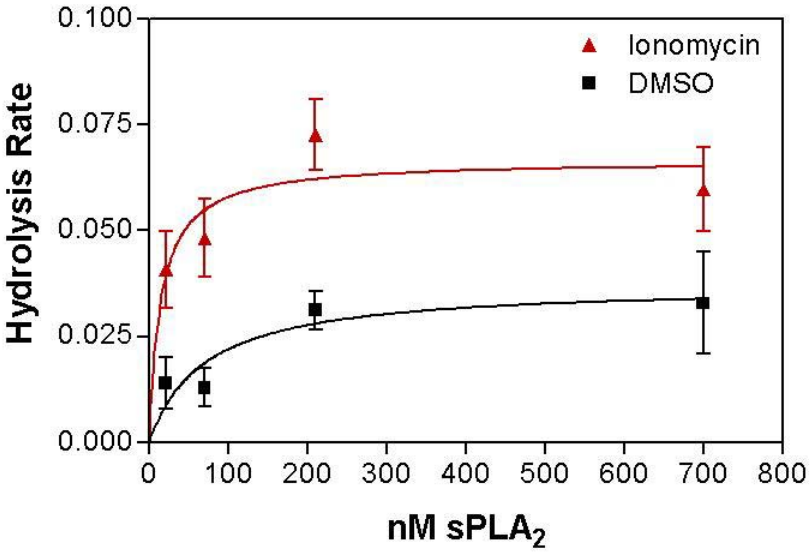
Hydrolysis Rate
0.100
0.075
0.050
0.025
0.000
0
100
200
300
400
500
600
700
800
nM sPLA2
Ionomycin
DMSO

Figure 5

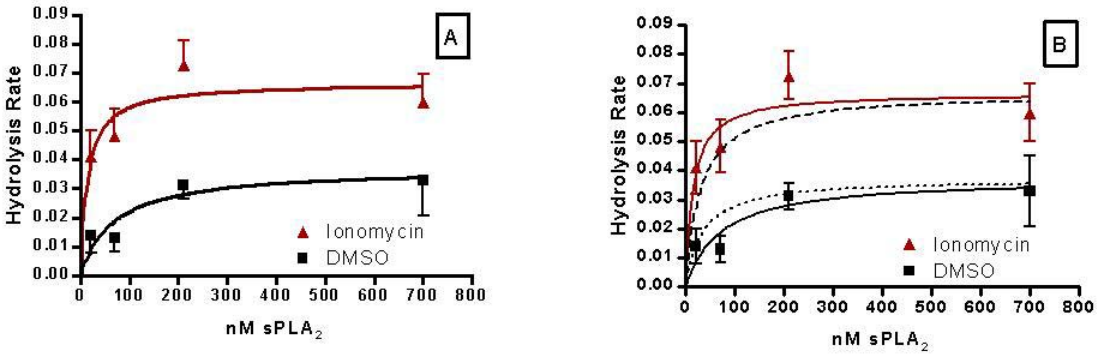
A
B
Hydrolysis Rate
0.09
0.08
0.07
0.06
0.05
0.04
0.03
0.02
0.01
0.00
0
100
200
300
400
500
600
700
800
nM sPLA2
Ionomycin
DMSO

Figure 6

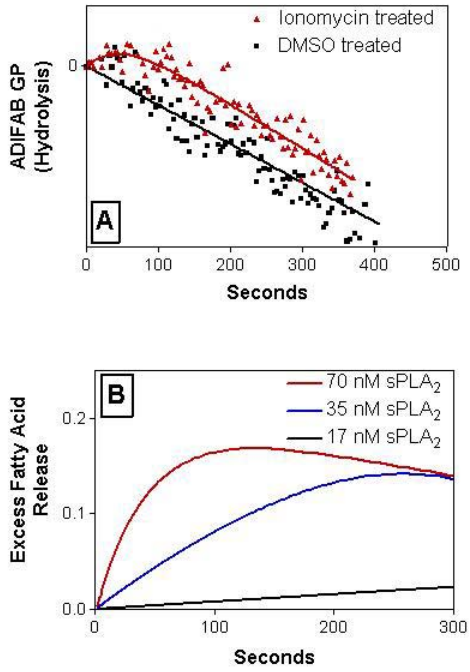
Ionomycin treated
DMSO treated
ADIFAB GP (Hydrolysis)
0
A
0
100
200
300
400
500
Seconds
B
70 nM sPLA2
35 nM sPLA2
17 nM sPLA2
Excess Fatty Acid Release
0.2
0.1
0.0
0
100
200
300
Seconds

Figure 7

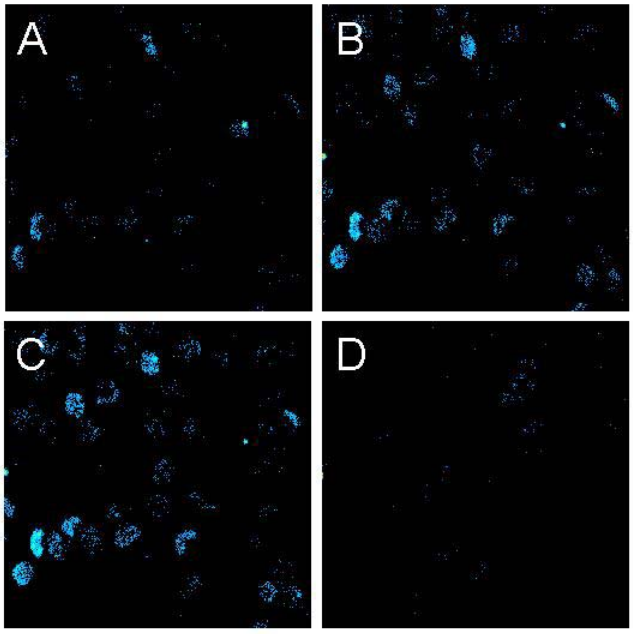

Figure 8

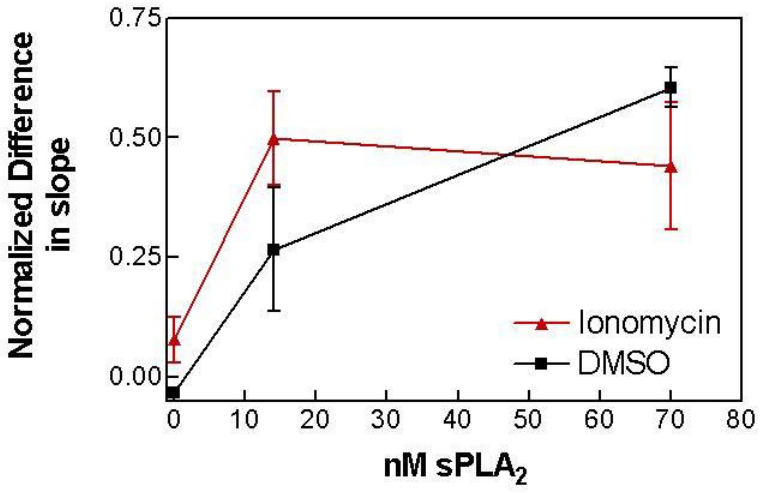
Normalized Difference in slope
0.75
0.50
0.25
0.00
0
10
20
30
40
50
60
70
80
nM sPLA2
Ionomycin
DMSO